JOURNAL OF CATALYSIS 44, 183–196 (1976)

Thermal Decomposition of Methanol Adsorbed on Alumina[1]

T. MATSUSHIMA AND J. M. WHITE

Department of Chemistry, University of Texas, Austin, Texas 78712

Received February 26, 1976

The kinetic behavior of methanol adsorbed on alumina powder was studied by thermal desorption and isotopic tracer techniques using an ultrahigh vacuum system. Several products were desorbed; CH_3OH is predominant at low temperatures, H_2CO, H_2O, and CH_3OCH_3 become significant at 500°K and higher, CO and CH_4 are observed above 700°K (CO predominates), H_2 is desorbed at both low and high temperatures peaking with H_2CO and CO, and finally CO_2 is observed in small amounts at all temperatures.

The isotopic composition of ethers desorbed after coadsorption of CH_3OH and CD_3OD was investigated. Below 500°K, only CH_3OCH_3, CD_3OCH_3, and CD_3OCD_3 appeared, while above this temperature the deuterium in ethers approached a random distribution. From this result it is concluded that below 500°K, adsorbed methanol (methoxide) is stable with respect to hydrogen exchange whereas at higher temperatures the H for D exchange is facile.

In the presence of gas phase CD_3OD, thermal desorption was examined from CH_3OH-preadsorbed substrate. The ether produced was primarily CH_3OCH_3 suggesting that ether is formed through the interaction of two adsorbed methoxides. The reactivity of adsorbed methoxides is discussed and it is suggested that heterogeneity is induced by adsorption and/or desorption.

INTRODUCTION

The dehydration of alcohols over alumina has been investigated kinetically under relatively high pressures by many workers (*1–9*). Several different reaction mechanisms, including both Eley–Rideal (*2, 8*) and Langmuir–Hinshelwood (*3, 9*), have been proposed. Infrared (*9–16*) and NMR (*17*) spectroscopy have been used to elucidate the adsorbed species formed during alcohol adsorption. Three surface species have been identified: (1) a weakly bound species having an alcohol structure, (2) a surface alkoxide chemisorbed species, and (3) a carboxylate chemisorbed species formed when alumina is heated to temperatures greater than 443°K.

The kinetic behavior of the adsorbed species has been studied using infrared spectroscopy (*9, 13–15*). While thermal decomposition and/or desorption of chemisorbed species provides considerable information about the kinetic behavior of the system, this technique has not been used in low pressure work on the alcohol dehydration, with the exception of one low resolution study of ethanol on alumina (15).

Since Al_2O_3 is an insulator and a poor thermal conductor, homogeneous heating of the sample is a serious experimental problem even for fine powder samples. The purposes of this work are to establish a method for heating homogeneously a small amount of alumina powder in an ultrahigh vacuum system, to determine the relative amounts of desorbed species as a function of substrate temperature, and to examine the kinetic behavior of species resulting from the adsorption of methanol on alumina.

[1] Supported by the Office of Naval Research.

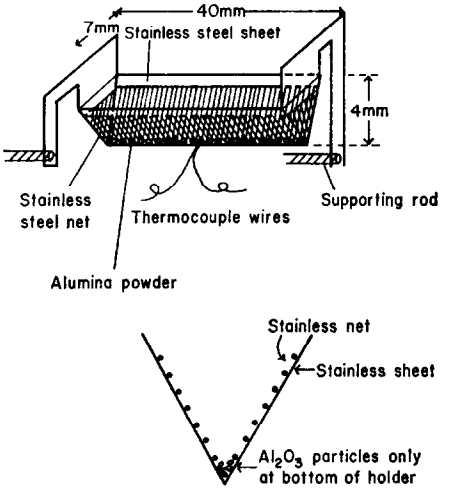

FIG. 1. Sample holder used for heating Al_2O_3 powder.

EXPERIMENTAL

Reaction system. The system was a bakeable ultrahigh vacuum apparatus such that the base pressure achieved was less than 2×10^{-7} Pa. During experimentation the system was continuously pumped by two ion pumps. The total pressure was monitored by measuring the current from the smaller ion pump, calibrated using a Bayard–Alpert type ionization gauge, while relative partial pressures were measured with a quadrupole mass spectrometer. Adsorbate vapors were admitted through leak valves.

Sample holder. A small double-walled V-shaped stainless steel (Type 302) basket, depicted in Fig. 1, was used to heat the substrate homogeneously in the vacuum system. It was constructed with an outer wall of sheet and inner wall of net and was connected via supporting stainless steel rods to the vacuum wall. A thermocouple was spot-welded to the bottom of the basket. The powdered alumina was screened into the netted portion in such a way that particles were trapped in the interstices of the netting.

In order to account for the influence of the sample holder on the observations, a replica holder without Al_2O_3 was placed in the system at a position with respect to the pumps and mass spectrometer that was equivalent to the position of the actual sample holder.

Alumina substrate. The sample was comprised of about 1.5 mg of 100–200 mesh powdered alumina, with a surface area of about 3×10^3 cm^2 (AlCO type F20). Prior to being incorporated into the holder, the alumina was heated in air at 823°K for 6 hr. After cooling, the sample was placed in the holder and heated to 1100°K under vacuum until the background pressure dropped below 5×10^{-6} Pa (about 2 hr of heating was required). Following this procedure, the temperature was lowered to 300°K and methanol vapor was admitted through one of the variable leak valves. After a certain exposure, the methanol flow was terminated and the sample was heated to 1100°K with pumping for 30 min and cooled to 300°K for 30 min. This last heating–cooling procedure was performed to each measurement described below.

Exposure of methanol and heating. During exposure of methanol, the filament of the quadrupole mass spectrometer was not operated in order to minimize the decomposition of methanol. Methanol gave six major mass-spectrometer peaks, at masses 2(H_2^+), 15(CH_3^+), 28(CO^+), 29-(HCO^+), 31(CH_2OH^+), and 32(CH_3OH^+). The ratios of mass 31 to the other masses, except masses 2 and 28, were independent of methanol pressure. The ratios of masses 28 and 2 to mass 31 decreased with increasing pressure and showed some time lag after the pressure was increased. These facts show that methanol decomposes on hot filaments to produce CO and H_2, as observed in other studies (*18, 19, 20*). The extent of decomposition varied with time after a step increase in methanol pressure; the CO peak increased by about 50%

during the approach to steady state. Operation of the ionization gauge caused about 20% of the methanol to decompose, making it impossible to operate the gauge for any measurement involving methanol. Therefore, this gauge was used only for the calibration of the current reading of the small ion pump which operated at room temperature. Back diffusion of decomposed species from the other (large) ion pump can be neglected.

In a preliminary test, the rate of heating the substrate alumina was varied from about 20°K min^{-1} up to 140°K min^{-1}. The thermal desorption spectra did not change, indicating that the substrate was heated homogeneously, as discussed below from another point of view. In the measurements described below, the heating rate was always near 140°K min^{-1}.

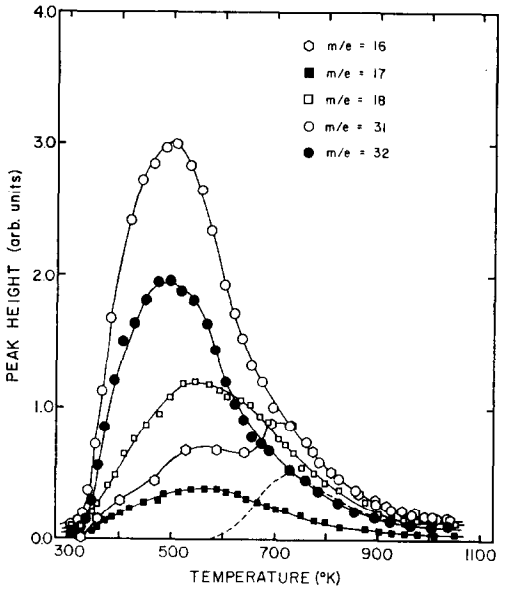

FIG. 2. Temperature variation of mass spectrometer signals at m/e = 16–18 and 31, 32. The data were generated by heating at 140°K min^{-1} an alumina substrate which has been exposed to 5×10^{-3} Pa of CH_3OH for 15 min and then evacuated for 30 min. The signals at m/e = 31 and 32 are assigned to methanol while those at 17 and 18 are assigned to water. The m/e = 16 peak is composed of contributions from H_2O, CH_3OH, and CH_4. The dashed curve which carries no symbol is the m/e = 16 signal after subtraction of the H_2O and CH_3OH contributions and is assigned as CH_4.

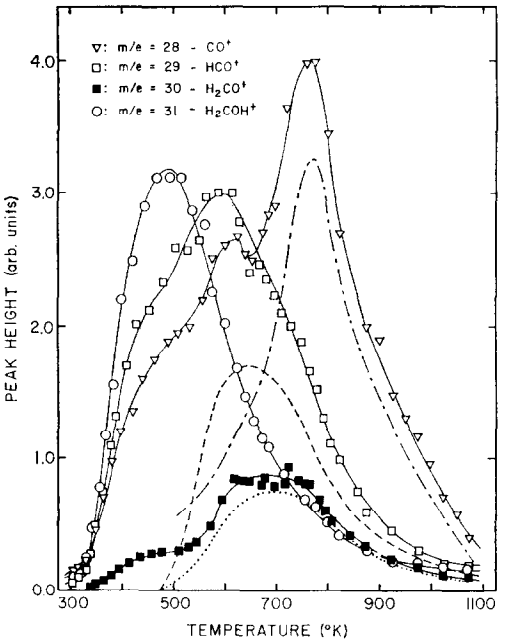

FIG. 3. Variation with temperature of masses belonging to CH_3OH, H_2CO, and CO during thermal decomposition of adsorbed methanol. The conditions are the same as for Fig. 2: 5×10^{-3} Pa of CH_3OH for 15 min, followed by evacuation for 30 min, and then heating at 140°K min^{-1}.

Adjusted m/e = 28–30 signals are as follows: — — —, m/e = 28 after subtraction of contributions due to CH_3OH and H_2CO; - - - -, m/e = 29 after correction for contributions arising from CH_3OH; · · · ·, m/e = 30 after correction for CH_3OH contributions. The resulting 28 signal is assigned to carbon monoxide, and the resulting 29 and 30 signals are assigned to formaldehyde.

RESULTS AND DISCUSSION

Desorbed Species

The results of one typical set of experiments are shown in Figs. 2–5. The substrate was exposed to 5.0×10^{-3} Pa of methanol for 15 min at room temperature. After evacuation for 30 min, the substrate was heated at the rate of about 140°K min^{-1}, while the gas phase was monitored. In the mass spectra, peaks due to H_2, CH_4, H_2O, CO, H_2CO, CH_3OH, CO_2, and CH_3OCH_3 were found. Thermal desorption

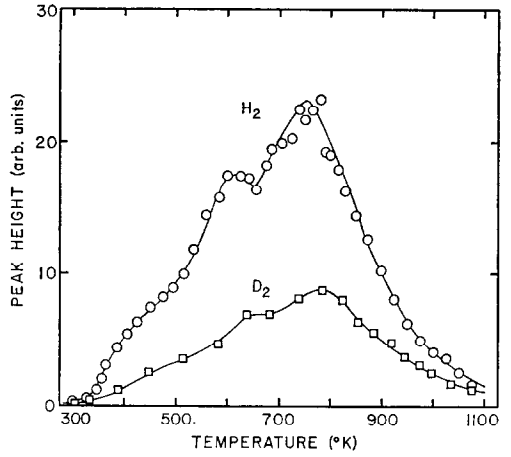

FIG. 4. Variation with temperature of H_2 after exposure at 5×10^{-3} Pa of CH_3OH for 15 min, evacuation for 30 min, and heating at 140°K min^{-1} (open circles). Open squares are for same exposure of CD_3OD. Lower temperature peak is associated with conversion of methoxide to formate species on the surface, while the higher temperature peak is associated with the decomposition of the adsorbed species (methoxide and formate). The lower intensity D_2 signal reflects an isotope effect in the chemisorption of methanol.

from the sample holder was negligibly small as established by heating the replica holder.

Methanol. The variation with the temperature of $m/e = 31$ and 32 is shown in Fig. 2. The ratio of these masses was the same at all temperatures in the range 350–1000°K, and agreed with the reported fragmentation pattern of methanol. These peaks were shifted to $m/e = 34$ and 36 when the substrate was exposed to CD_3OD. Therefore, both masses 31 and 32 were assigned to methanol.

The desorption of methanol started around 350°K and showed a maximum near 500°K and a slow decline to background levels by the time the temperature reached around 950°K.

Water. Figure 2 shows the temperature variation of $m/e = 17$ and 18, which are due to water. The peak maximum temperature is near that for ether (see Fig. 5), but the desorption spectrum was much broader than that of ether and started at lower temperatures. The water spectrum is consistent with water adsorption data on Al_2O_3 (*21*, *22*). It should be noted that the amount of H_2O desorbed is generally larger than that of ether, probably because a trace of water (less than 0.1%) in the methanol was adsorbed and desorbed.

Methane. Mass 16 shows two peaks, as shown in Fig. 2. Methanol contributes to the $m/e = 16$ peak to the extent of 15% of $m/e = 31$ peak. Water also contributes to $m/e = 16$ (a few percent of $m/e = 18$ peak). The dashed curve in Fig. 2 shows $m/e = 16$ corrected for these contributions from water and methanol and was identified as CH_4. Methane desorbed around 600°K and peaked around 730°K. Methane was reported in thermal decomposition of aluminum methoxide (*23*).

Formaldehyde. The variation of masses 28 through 31 is shown in Fig. 3. The dashed and dotted lines show $m/e = 29$ and 30 after correcting for methanol contributions. The resultant ratio of m/e

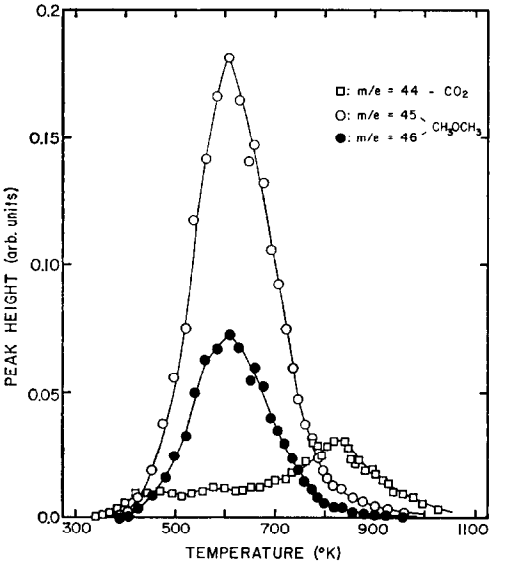

FIG. 5. The temperature dependence of ether ($m/e = 45$ and 46) and carbon dioxide ($m/e = 44$) production from an alumina substrate exposed to 5×10^{-3} Pa of CH_3OH for 15 min, evacuated for 30 min, and then heated at 140°K min^{-1}.

= 29 to m/e = 30 is almost constant over the entire temperature range, and is in general agreement with the literature value for the fragmentation of formaldehyde. In addition, these masses were shifted to m/e = 30 and 32 when CD_3OD was used. Thus, we assign these corrected signals to formaldehyde.

The desorption of formaldehyde is not important at temperatures below 500°K, but makes an important contribution between 500 and 900°K, with maximum production near 650°K. This agrees well with other work. According to infrared spectroscopic results (*10–14*), surface methoxide is converted to formate ion above 443°K. The formate ion is decomposed around 773°K (*11*). The decomposition of methanol on the stainless steel sample holder produces a negligibly small amount of formaldehyde.

Carbon monoxide. The largest dotted–dashed peak in Fig. 3 shows mass 28 after corrections for contributions from methanol and formaldehyde to the observed m/e = 28. This peak was not shifted when CD_3OD was used. Therefore, it is not ethylene, as observed in thermal decomposition of bulk aluminum methoxide (*23*).

Decomposition of methanol on the mass spectrometer filament produces CO, as mentioned above, and the amount is relatively significant at low substrate temperatures, but becomes small at temperatures above 650°K where the gas phase methanol pressure is relatively low. The CO maximum around 770°K is due to thermal decomposition of adsorbed species on Al_2O_3. Above 900°K, CO is the predominant desorbed species.

Hydrogen. The thermal desorption of hydrogen (m/e = 2) or deuterium (m/e = 4) from CD_3OD adsorption, shows two peaks at 610 and 760°K as illustrated by Fig. 4. The lower temperature peak is at the same temperature as the formaldehyde peak (*11*, *23*) and the higher is at the same temperature as the CO peak position. These results suggest that hydrogen is one product of the reactions of surface species which lead to formaldehyde or carbon monoxide. A small shoulder below 500°K in Fig. 4 may be due to the fragmentation of methanol.

Dimethyl ether. The data related to dimethyl ether, CH_3OCH_3, are shown in Fig. 5 as curves for masses 45 and 46. Ether production is significant at temperatures below those where formaldehyde becomes important. At high temperatures ether formation is quite small compared to formaldehyde. The largest ether production occurs near 600°K. When CD_3OD was adsorbed, deuterated dimethyl ether (CD_3OCD_3) is desorbed, as shown in Fig. 6 as curves for masses 50 and 52.

Carbon dioxide. Carbon dioxide (m/e = 44) is shown in Figs. 5 and 6. It was not shifted even when CD_3OD was used. The predominant high temperature peak follows a temperature profile similar to that of carbon monoxide which suggests that a certain fraction of the CO produced is oxidized to CO_2.

Adsorption and Desorption Rates of Methanol

The coverage of CH_3OH was estimated from thermal desorption spectra of mass 31 (CH_2OH^+), assuming the relative peak heights of all desorbed species to be constant. This is an approximation since the desorption of ether increased more than methanol as the coverage increased; however, ether was always less than 20% of methanol.

Figure 7a shows the relative coverage of methanol as a function of methanol exposure at 300°K and 5×10^{-3} Pa. After exposure and before thermal desorption the system was evacuated for 30 min. The coverage increased linearly at low exposure times and reached saturation at about 1 hr. The dependence of coverage on evacuation time after a fixed exposure (5×10^{-3} Pa

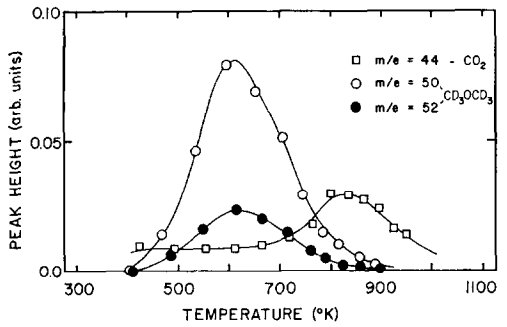

FIG. 6. The temperature dependence of the production of deuterated ether (m/e = 50 and 52) and carbon dioxide (m/e = 44) from an alumina substrate exposed to 5×10^{-3} Pa of CD_3OD for 15 min, evacuated for 30 min, and heated at 140°K min^{-1}. Although the amount of deuterated ether is generally smaller than nondeuterated after the same exposure (see Fig. 5), the temperature at which the rate peaks is very nearly the same.

$\times$ 20 min), is shown in Fig. 7b. Clearly, adsorbed methanol is desorbed very slowly at 300°K.

Regardless of the initial amount of methanol adsorbed at 300°K (methoxide as discussed below), desorption of methanol and ether started around 350 and 375°K, and showed the maxima around 500 and 600°K, respectively. It should be noticed that desorption began at the same temperature even for coverages below 3% of the maximum coverage, although the spectrum became very broad.

Desorbed Species Resulting from Coadsorption of CD_3OD and CH_3OH

In a series of isotope tracer experiments the structure and reactivity of adsorbed species were probed by examining the deuterium distribution of methanols and ethers desorbed following coadsorption of CH_3OH and CD_3OD.

Ether. The adsorption of either CH_3OH or CD_3OD, but not both, gave the desorption results presented in Figs. 5 and 6. When CH_3OH alone was used, the ratio of m/e = 45 to m/e = 46 was constant over the entire temperature range, and signals at m/e = 47–52, belonging to isotopically labeled ethers, were absent. The areas under the desorption profiles of CD_3OCD_3 (Fig. 6) and D_2 (Fig. 4) were always smaller than areas for CH_3OCH_3 and H_2 measured under conditions of equal exposure. The difference is attributable to an isotope effect on the rate of methanol adsorption which favors CH_3OH.

The desorption of ether after coadsorption of CH_3OH and CD_3OD is summarized in Fig. 8. The procedure was as follows. First CH_3OH was admitted for 15 min at a constant pressure of 5×10^{-3} Pa and 300°K; the system was then evacuated for 15 min, after which CD_3OD was admitted at a constant pressure of 5×10^{-3} Pa for 15 min; the system was then evacuated for 30 min at 300°K prior to beginning the thermal desorption study. The temperature variation of each mass number belonging

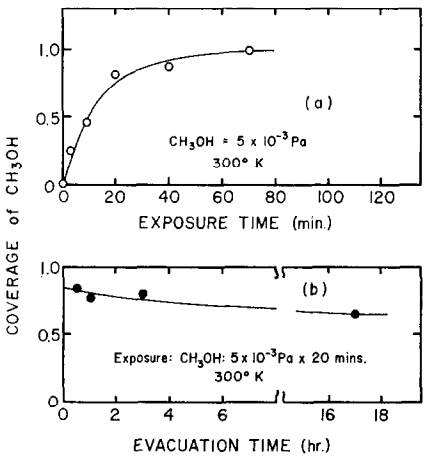

FIG. 7. (a) The dependence of the amount of desorbed methanol on the exposure. Methanol was adsorbed for various times at 5×10^{-3} Pa and 300°K, evacuated for 30 min, and then heated at 140°K min^{-1}. The coverage was estimated from the area under the desorbed methanol peak and the results were normalized to unit coverage at an exposure time of 70 min. (b) The dependence of the amount of desorbed methanol on the length of the evacuation period after adsorption. The exposure was held constant at 5×10^{-3} Pa, 20 min, and 300°K. The data are normalized to the 70-min exposure time (saturated) adsorption of Fig. 7a.

to ether, $m/e = 45$ through 52, is shown in Fig. 8. The highest amplitude solid curve shows the total ether pressure, which is the summation of all mass amplitudes divided by the fragmentation factors, normalized to the fragment $CH_3OCH_2^+$. The result is essentially the same as the $m/e = 45$ or 50 obtained when either CH_3OH or CD_3OD was adsorbed alone. However, in coadsorption, each mass shows a different onset temperature and different maximum position. This means that the deuterium distribution in the ethers depends upon the substrate temperature; i.e., the isotopic composition of ether, CH_3OCH_3, CH_2DOCH_3, CHD_2OCH_3, $\cdots$, CD_3OCD_3, varies with the temperature.

It should be noticed that mass 51, which can arise only from CD_3OCD_2H, first appeared around 510°K, and that the ratios of $m/e = 45$ to 46 and $m/e = 50$ to 52 were constant below 510°K. These ratios are the same as those measured when the

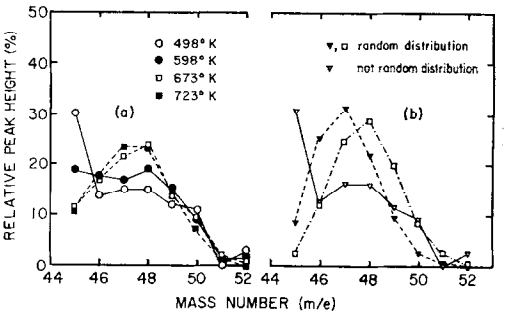

FIG. 9. (a) Relative peak heights of isotopic ethers at various temperatures following coadsorption of CH_3OH and CD_3OD (15-min exposure of each at 5×10^{-3} Pa). Note the shift away from low and high masses as the temperature is raised. (b) Computed mass distribution of ether peaks for various conditions. ▽, Nonrandom deuterium distribution (i.e., CH_3OCH_3, CD_3OCH_3, and CD_3OCD_3 only) for a deuterium fraction of 0.35. □, ▼, Random deuterium distribution among isotopic ethers assuming 0.5 and 0.35 deuterium fraction, respectively. Comparing (a) and (b) shows a definite nonrandomness in isotopic distribution for $T < 600$°K and nearly random distribution for $T \geq 670$°K.

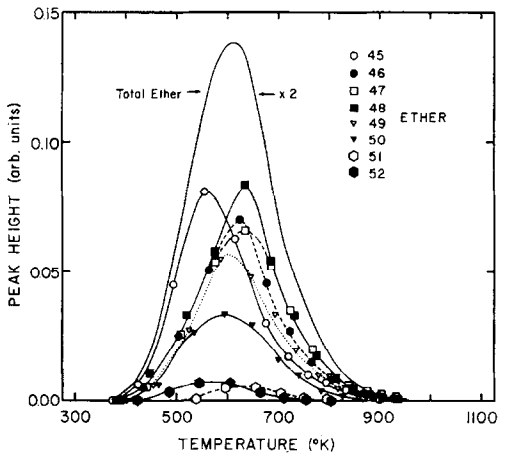

FIG. 8. The temperature dependence of the desorption of various isotopic ethers following coadsorption of CH_3OH and CD_3OD. Nondeuterated methanol was admitted for 15 min at 300°K and 5×10^{-3} Pa, the system was evacuated for 15 min. CD_3OD was admitted for 15 min at 5×10^{-3} Pa, the system was evacuated for 30 min, and then heated at 140°K min^{-1}. Note that $m/e = 51$, which comes from only $CHD_2OCD_3^+$, appears only above 510°K and serves as a marker for the onset of hydrogen atom exchange among the methyl groups.

only product is either CH_3OCH_3 or CD_3OCD_3. These facts suggest that below 510°K, methanol, adsorbed as CH_3O(a) or CD_3O(a), is stable (if methoxide is dissociated, the reverse reaction does not occur), and that no exchange of hydrogen occurs among adsorbed methoxide or hydrogen. Thus, desorbed ether contains only CH_3OCH_3, CH_3OCD_3, and CD_3OCD_3, but not the other isotopic ethers. Above this temperature, hydrogen exchange becomes fast and D is mixed with H in the methyl groups.

In order to discuss this point more clearly, the relative peak heights at various temperatures are shown in Fig. 9a. Below 510°K, the relative peak heights are almost constant independent of the temperature. Above 673°K, the distribution of masses was quite different from that at 498°K; masses 52 and 45 decreased very much, whereas masses 47 and 48 increased. Eventually, the curve became bell-shaped. Below 510°K, masses 45 and 46 and masses

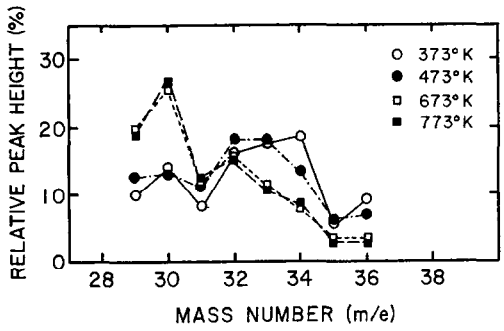

FIG. 10. Relative peak heights of masses due to isotopic methanol molecules after coadsorption of CD_3OD and CH_3OH (5×10^{-3} Pa, 15 min, 300°K each). Note, that at low temperatures there is a significant mass 35 peak arising from CD_3OH.

50 and 52 can be assigned to CH_3OCH_3 and CH_3OCD_3, respectively, as discussed above. CH_3OCD_3 produces masses 47, 48, and 49. The ratio of the sum of masses 47 and 48 to mass 49 lies between the ratios of $m/e = 45$ to 46, and $m/e = 50$ to 52. Therefore, it is reasonable that $m/e = 47$, 48, and 49 be assigned to CH_3OCD_3. Accordingly, desorbed ether below 510°K contains only CH_3OCH_3, CH_3OCD_3, and CD_3OCD_3.

Above 673°K, mass 51 appeared and mass 45 was smaller than mass 46. This mass distribution cannot be explained by any mixture of CH_3OCH_3, CH_3OCD_3, and CD_3OCD_3. It suggests that ether produced at higher temperatures involves the scrambling of D and H in the methyl groups.

Assuming that the isotope effect on the ether mass spectrum fragmentation pattern is small, the relative peak heights can be calculated when deuterium is distributed in ether at random. Mass distributions calculated for deuterium fractions of 0.35 and 0.5 are shown in Fig. 9b. The triangles show the distribution expected when ether contains only CH_3OCH_3, CH_3OCD_3, and CD_3OCD_3, and the deuterium fraction of 0.35. This curve is quite similar to that observed at 498°K.

The relative peak heights calculated, assuming a random distribution, are quite similar to the experimental data above 673°K. A small discrepancy exists between them and may be due to the assumptions of no isotope effect and fully random distribution.

At 598°K, Fig. 9a shows that the experimental distribution is intermediate between fully random and nonrandom. From this we conclude that the hydrogen exchange rate at this temperature is not fast enough to generate a random hydrogen isotope distribution.

It is clear from the above discussion that the CH_3 group in adsorbed methoxide is stable below 510°K, with respect to hydrogen exchange, and that above 510°K the hydrogen exchange becomes significant. The relation of this exchange reaction to

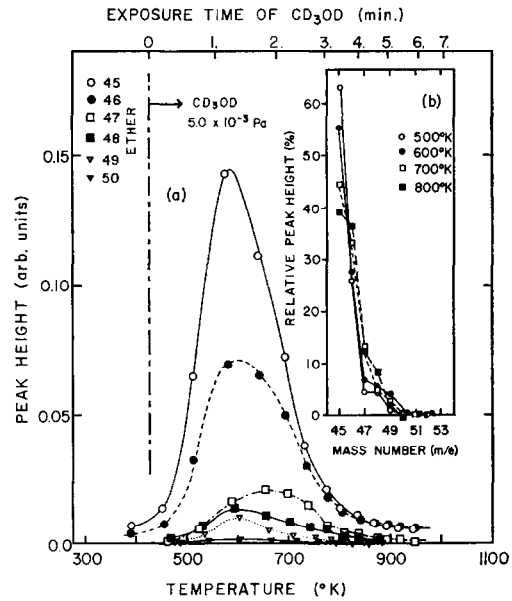

FIG. 11. (a) Temperature dependence of isotopic ether mass spectra after adsorption of CH_3OH at 300°K and 5×10^{-3} Pa for 45 min and evacuation for 4 hr. The substrate was heated at 140°K min^{-1}, and, at 425°K, CD_3OD was introduced at a pressure of 5×10^{-3} Pa. Note the relatively small contribution of deuterated methanol. (b) Mass distributions at various temperatures from Fig. 11a emphasizing the dominance of nondeuterated ether under conditions where CD_3OD predominates in the gas phase and CH_3O(a) predominates in the adsorbed phase.

the formation of adsorbed formate is not clear.

The effect of the sample holder on the hydrogen exchange process was confirmed to be negligibly small by heating the replica holder in the presence of isotopically mixed ethers.

Methanol. Figure 10 shows the experimental distribution of masses 29 through 36 belonging to isotopic methanol species desorbed after CH_3OH was exposed for 15 min (5×10^{-3} Pa) and followed with the same exposure of CD_3OD using the procedure outlined above. As discussed above, the methyl group of the adsorbed methanol does not contain the other hydrogen isotope below 510°K. Therefore, below 473°K, mass 35 (shown in Fig. 10) should arise only from CD_3OH. The distribution below this temperature can be explained, assuming only CH_3OH, CH_3OD, CD_3OH, and CD_3OD. Therefore, we conclude that methanol is adsorbed dissociatively in agreement with ir studies (*9–14*), which showed methanol to be adsorbed as methoxide, CH_3O.

On the other hand, the distribution above 673°K cannot be explained, even if we assume a random deuterium distribution. The reason is that formaldehyde contributes to masses less than 32 and the corrections are difficult to make and to retain any experimental certainty.

Ether Formation Mechanism

In this section we present experimental data which confirm that ether is formed by the decomposition of surface methoxide groups and that gas phase methanol colliding with surface species plays no significant role in ether formation.

With the substrate at 300°K, CH_3OH at 5×10^{-3} Pa was admitted to the system for 45 min. After evacuation for 4 hr, a thermal desorption cycle was begun and when the temperature reached 423°K, CD_3OD was admitted to the system at a constant pressure of 5×10^{-3} Pa while heating continued. During this period the ether masses were monitored, and the results are displayed in Fig. 11. The temperature profiles and mass distributions of Fig. 11a and b show that $m/e = 45$ and 46 predominate below 600°K, indicating that CH_3OCH_3 is the predominant ether even though CD_3OD predominates in the gas phase. Mass spectrometer signals from $m/e = 47$–52 are either small or absent at these temperatures.

Above 600°K, $m/e = 45$ and 46 still predominate the spectrum but the ratio of these signals does not fit the fragmentation pattern of CH_3OCH_3. Further, a larger amount of deuterium is incorporated into the observed species, and it is (as Fig. 11b shows) distributed randomly over the various species. Thus, a small amount of CD_3OD is adsorbed and is involved in ether production, but the entire amount of ether produced is best accounted for by a reaction between two adsorbed methoxide species in a Langmuir–Hinshelwood type reaction in agreement with earlier work at high pressures by Tamaru and co-workers (*9*). In this context, it is important to note that when CH_3OH was preadsorbed, its pressure during the thermal desorption cycle was always less than 5% of the CD_3OD pressure. When the order of admission of the isotopic methanols was reversed, CD_3OCD_3 was the predominant ether.

Reactivity of Adsorbed Methoxide

Arai *et al.* (15) reported the thermal decomposition of ethanol adsorbed on alumina showing that at low temperatures the product was primarily ethanol, at intermediate temperatures diethyl ether was predominant, and at high temperatures ethylene was a major product. They explained the temperature dependence of the products by considering various strengths of aluminum–oxygen (in ethoxide) binding. However, Tamaru and co-workers (*9*) suggested, on the basis of kinetic data,

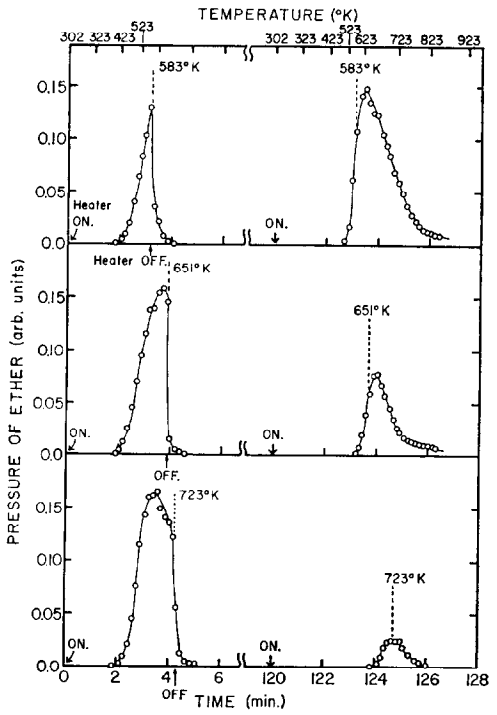

FIG. 12. Ether desorption profiles after adsorption of CH_3OH at 300°K and 5×10^{-3} Pa for 15 min. The left-hand portion of each panel shows the ether desorption profile when the sample was heated to T_s = 583, 651, and 723°K, respectively, after which the heater was turned off while pumping continued for 2 hr. The sample was then heated again at a rate of 140°K min^{-1}, and the ether desorption profile is shown in the right-hand half of each panel. Note that the major part of the second desorption occurs only after the temperature of the first heating is exceeded, except at 723°K.

that the methoxides behave uniformly in the working state. This point was examined for methanol as follows.

Ether formation. After a 15-min exposure of CH_3OH (5×10^{-3} Pa) at 300°K, the substrate was heated at a rate near 140°K min^{-1} to a desired temperature, T_s. At this point the heating was stopped and the substrate temperature returned to 300°K. After 2 hr, the substrate was again heated at the same rate to 900°K. During this procedure, masses 31 (CH_2OH^+) and 45 ($CH_3OCH_2^+$) were monitored. Figure 12 shows results for ether at various values of T_s. Notice that desorption decreased immediately upon termination of the first heating, and that ether was not produced during the second heating until the temperature approached T_s. When CD_3OD was adsorbed, the same behavior was observed for CD_3OCD_3 desorption.

If there is a distribution of methoxide binding energies such that various adsorbed methoxides require different critical temperatures in order to react relatively rapidly, then methoxides remaining after the first heating should neither react nor be desorbed below T_s. However, another experiment, outlined below, shows that even remnant methoxides can react and produce ether below T_s.

After the first heating following a CD_3OD exposure, CH_3OH at a pressure of 5×10^{-3} Pa was admitted for 15 min,

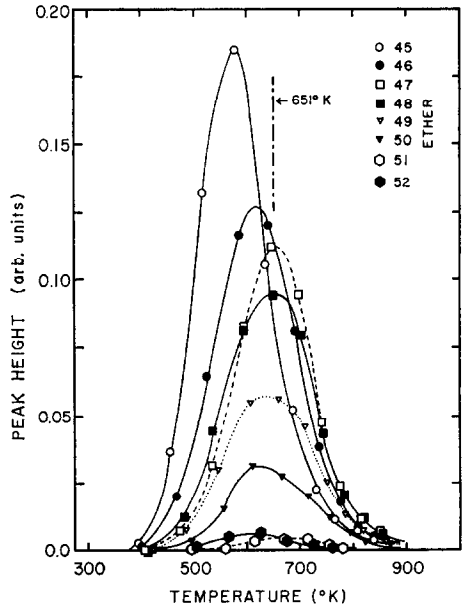

FIG. 13. Temperature profiles of mass spectrometer signal corresponding to various isotopic ethers formed from remnant CD_3O(a) and newly adsorbed CH_3OH. The CD_3OD was adsorbed first, the sample was heated to 651°K to partially desorb products, the CH_3OH was adsorbed at 300°K, and finally, the sample was heated to desorb products. Note the significant contribution of m/e = 47–49 below 650°K suggesting that remnant CD_3O(a) is available for reaction if a neighboring CH_3O(a) is present.

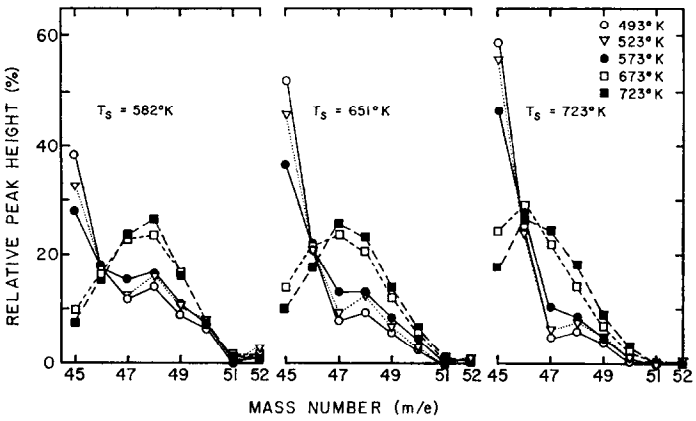

FIG. 14. Mass distributions of isotopic ethers formed from remnant $CD_3O(a)$ and $CH_3O(a)$ adsorbed after removal of some $CD_3O(a)$ with a preliminary heating to temperature T_s. After this removal, CH_3OH was adsorbed for 15 min at 300°K and the system was pumped for 1 hr before reheating the sample to give the spectra shown in this figure.

and then, after 1 hr evacuation, the substrate was reheated. Masses belonging to ether desorbed during the second heating are shown in Fig. 13. The peak distributions for various T_s are drawn in Fig. 14. The peak distributions below 523°K, at any T_s, can be assigned to mixtures of CH_3OCH_3, CH_3OCD_3, and CD_3OCD_3.

Above 673°K, the peak distributions show the random distribution of deuterium in ether. The deuterium content in the ether decreased with increasing T_s, since the amount of remnant $CD_3O(a)$ decreased with T_s. It should be noticed that the ether desorbed below T_s contains a significant amount of CH_3OCD_3 and a small amount of CD_3OCD_3, as shown in Fig. 13. The relative abundance of CH_3OCH_3, CH_3OCD_3, and CD_3OCD_3 below 523°K corresponds to a random distribution of CH_3 and CD_3 groups. This fact indicates that the remnant methoxides left after the first heating behave kinetically like the methoxides added at 300°K after the first heating; i.e., there is no difference in reactivity between the remnant and the added methoxides. The results of these experiments also confirm that the substrate was heated homogeneously since non-uniform heating would preferentially deplete the species added after the first heating cycle.

Methanol. Similar phenomena were observed for methanol which also started to desorb around T_s during the second heating. As discussed below, when the sample was exposed at 300°K to methanol between the first and second heating, methanol desorbed below T_s during the second heating contained a significant amount of methoxide left after the first heating.

After the first heating (T_s = 623°K) following a CD_3OD exposure, CH_3OH was admitted and then the substrate was heated in the manner described above for ether analysis. Masses greater than m/e = 31 belonging to methanol are shown in Fig. 15. As indicated above, methyl groups desorbed below 510°K contain only CH_3 and CD_3. Using the fragmentation patterns of methanol (*24*, *25*), the major masses from CH_3OH, CD_3OH, CH_3OD, and CD_3OD are m/e = 32 and 31, 35 and 33, 33 and 32, and 36 and 34, respectively. Every former mass is 70 to 80% of the latter. Therefore, it can be seen from Fig. 15 that methanol desorbed at 423 and 523°K contains mainly CH_3OH and CH_3OD. In addition, CD_3OH is significant while CD_3OD is very small. This fact suggests that remnant $CD_3O(a)$ left after the first heating can be desorbed readily below T_s provided there

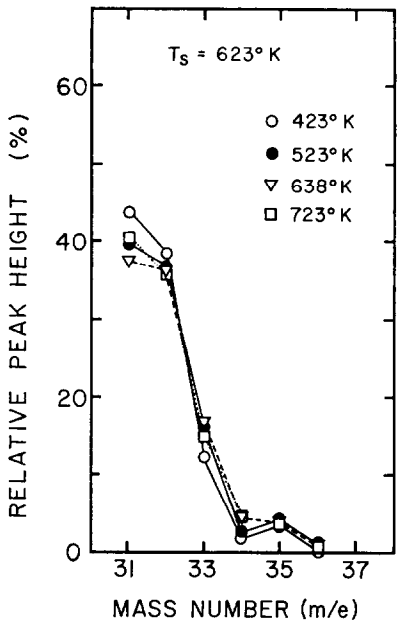

FIG. 15. Mass distributions of desorbed isotopic methanol molecules formed from remnant CD_3O(a) and adsorbed methanol. After heating a sample, which had been exposed to CD_3OD, to a temperature of 623°K, the substrate was returned to 300°K and exposed to CH_3OH. After exposure and pumping, the substrate was heated again to give the above spectra. Note the significant contribution of m/e = 35 and 33 arising from CD_3OH.

is a second exposure at 300°K. Above 638°K, the deuterium distribution becomes random and the desorbed methanol contains all the deuterium-substituted groups.

Discussion of the reactivity. The behavior of the methanol and ether desorption curves under various conditions is very interesting. For both methanol and ether, the experiments which involve two heating cycles with no adsorption between seem to suggest, because of the strong shift of the onset temperatures, a variation with coverage of the overall activation energy. On the other hand, the results for a single desorption cycle, after exposures giving coverages varying by a factor of 30, are all characterized by the same onset temperature and same peak temperature for methanol desorption. In these same experiments, the onset temperature for ether desorption is also independent of surface coverage.

If the two-cycle experiments involve an activation energy depending only on the total coverage of certain absorbed species, the single-cycle data should show an onset temperature which declines as the coverage increases.[2] Since this is not observed, it is necessary to treat the one-cycle experiments and the second cycles of the two-cycle experiments as having different distributions among the states available to a given species. This becomes even more apparent when, at equal coverages, a single-cycle experiment is compared with the second cycle of a two-cycle experiment.

It is not possible to apply directly the usual second-order desorption treatment (*26*, *27*) to the data reported here because new reaction paths become important as the temperature is increased.

The coverage dependence of the activation energy cannot be explained by intrinsic heterogeneity of adsorption sites because there is no difference in the reactivity of methoxide remaining after the first heating and that added by adsorption at 300°K between the first and second heating cycles. In other words, we cannot use a surface model involving strong and weak binding sites and for which the adsorbate is expected to absorb preferentially on strong binding sites and to desorb first from weak binding sites (*28*).

The heterogeneity in these samples appears to be induced by adsorption and/or desorption. This effect could arise from either repulsive interactions between adsorbed species or the variation in binding to the surface with the number of nearest neighbor adsorbed species. The latter might restrict the mobility of methyl group because of a deficiency of neighboring

[2] Even if the activation energy was independent of coverage, the onset temperature would tend to decline as the coverage increases because the minimum detectable rate would be realized at a somewhat lower temperature.

hydroxyl groups, and/or an increase of the binding energy as proposed by Peri in the case of water adsorption on Al_2O_3 (*29*). The variation in the mobility seems unlikely because the induced heterogeneity was observed even at very low coverage as mentioned in the section Adsorption and Desorption Rates of Methanol, under Results and Discussion.

With the following model, it is possible to rationalize the experimental data reported in the Experimental section. We assume that methoxides have very low mobility on Al_2O_3 and that adjacent pairs are required for methanol and ether formation (a methoxide and hydroxyl or hydrogen adatom to form methanol, and two methoxides to form ether). The hydroxyl groups may be any one of a number of kinds (*14, 22, 29*). The formation and desorption of both methanol and ether leave surface oxygen atoms behind which may contribute to surface heterogeneity. The fact that methanol and ether, rather than formaldehyde and carbon monoxide, are desorbed at relatively low temperatures suggests that the relative surface concentration of oxygen increases as desorption proceeds. At the same time, there is a reduction in the average number of those nearest neighbor species which lead to methanol or ether (*29*). We assume that the activation energy for methanol and ether formation increases as the average number of nearest neighbors decreases. Because diffusion of surface species is slow, there is little change in the surface configuration between the first and second heating of two-cycle experiments unless gas phase methanol is introduced in the intermediate period. We assume further that methanol adsorption occurs with some preference for island formation and that remnant and new adsorbed species participate equally.

With this model the initial adsorption, regardless of exposure, will result in a broad distribution of the number of nearest neighbor species, including pairs that react and desorb as products with low activation energy. Thus, the onset temperature will be independent of initial coverage in the single-cycle experiments. Taking cognizance of the role played by competitive reactions and the distribution of nearest neighbors formed in the initial adsorption, one can account for the invariance of the peak temperatures for methanol and ether desorption. In the two-cycle desorption experiments with no intermediate adsorption, the strong shift of the onset temperature arises because of changes in the distribution of the number of nearest neighbors arising during the first heating cycle. In the first cycle, the products arise predominantly from those regions where the number of nearest neighbors is large. With no surface diffusion during the period between the two cycles, the distribution at the end of the first cycle is preserved and thus the second heating cycle involves a distribution characterized by a higher activation energy than the first cycle. As a result, the onset temperature is very nearly equal to T_s, the maximum temperature reached in the first cycle (Fig. 12). At relatively high temperatures, for example, at 723°K in Fig. 12, surface diffusion becomes fairly rapid, allowing a significant number of new pairs to be formed during the course of the heating cycle.

For those two-cycle experiments in which adsorption occurred between the cycles, a new distribution of the number of nearest neighbors was formed with remnant material and newly adsorbed material participating on an equal footing. Thus, the second cycle is characterized by a low onset temperature and, in the isotope tracer experiments, by random participation of CH_3 and CD_3 groups in methanol and ether formation.

CONCLUSIONS

The kinetic behavior of CH_3OH adsorbed on Al_2O_3 powder was studied by thermal

desorption and isotope tracer techniques, and the following conclusions are drawn.

(i) Methanol is desorbed at low temperatures. Near 500°K and above, H_2CO, H_2O, and CH_3OCH_3 become significant. Above 700°K, CO is predominant and CH_4 is significant. CO_2 is very small throughout the entire temperature range.

(ii) Adsorption and desorption rates of methanol are very small at 300°K, and CH_3OH adsorbs more rapidly than CD_3OD.

(iii) Ether desorbed after coadsorption of CD_3OD and CH_3OH contains only CH_3OCH_3, CH_3OCD_3, and CD_3OCD_3 below 510°K and the adsorbed methoxide is stable. Above this temperature the deuterium distribution in ether becomes random and hydrogen exchange between adsorbed methoxides occurs readily.

(iv) Thermal decomposition of preadsorbed CH_3OH in the presence of gas phase CD_3OD produces primarily CH_3OCH_3. Therefore, ether is formed primarily via a Langmuir–Hinshelwood reaction between two adsorbed adjacent methoxides.

(v) The methoxide remaining on Al_2O_3 at high temperatures can be desorbed or can react below this temperature after another exposure of methanol at 300°K. No difference was found among the reactivities of adsorbed methoxides; thus, intrinsic adsorption site heterogeneity is not significant in these experiments.

(vi) The production of both methanol and ether is qualitatively modeled by assuming heterogeneity of adsorption sites induced by adsorption and/or desorption, low surface mobility of surface species, and a Langmuir–Hinshelwood mechanism for the formation of desorbed products.

ACKNOWLEDGMENTS

The authors thank the members of our research group for continual interest and assistance in carrying out these experiments, and appreciate the work of Donna Jackson and Virginia Hale in preparing the manuscript. We are especially grateful to David Almy for his preliminary work on this project, and to David Foyt for helpful comments on the manuscript.

REFERENCES

1. Pines, H., and Manassen, J., *Adv. Catal.* **16**, 49 (1966).
2. deBoer, J. H., Fahim, R. B., Linsen, B. G., Visseren, W. J., and de Vleesschauwer, W. F. N. M., *J. Catal.* **7**, 163 (1967).
3. Jain, J. R., and Pillai, C. N., *J. Catal.* **9**, 322 (1967).
4. Wade, W. H., Teranishi, S., and Durham, J. L., *J. Phys. Chem.* **69**, 590 (1965).
5. Wade, W. H., Teranishi, S., and Durham, J. L., *J. Colloid Interface Sci.* **21**, 349 (1966).
6. Knözinger, H., Bühl, H., and Kochloefl, K., *J. Catal.* **24**, 57 (1972).
7. Knözinger, H., Kochloefl, K., and Meye, W., *J. Catal.* **28**, 67 (1973).
8. DeBoer, J. H., and Visseren, W. J., *Catal. Rev.* **5**, 55 (1971).
9. Soma, Y., Onishi, T., and Tamaru, K., *Trans. Faraday Soc.* **65**, 2215 (1969).
10. Greenler, R. G., *J. Chem. Phys.* **37**, 2094 (1962).
11. Kagel, R. D., *J. Phys. Chem.* **71**, 844 (1967).
12. Treibmann, D., and Simon, A., *Ber. Busenges. Phys. Chem.* **70**, 562 (1966).
13. Deo, A. V., and Dalla Lana, I. G., *J. Phys. Chem.* **73**, 716 (1969).
14. Hertl, W., and Cuenca, A. M., *J. Phys. Chem.* **77**, 1120 (1973).
15. Arai, H., Take, J., Saito, Y., and Yoneda, Y., *J. Catal.* **9**, 146 (1967).
16. Little, L. H., *in* "Infrared Spectra of Adsorbed Species," p. 176. Academic Press, London, 1966.
17. Kazanskii, V. B., and Borevkov, V. Yu., *Kinetika i Kataliz* **14**, 1193 (1973).
18. Roberts, M. W., and Stewart, T. I., *in* "Chemisorption and Catalysis" (P. Hepple, Ed.) p. 16. Elsevier Publishing Co., Amsterdam/New York, 1970.
19. Gasser, R. P. H., Roberts, K., and Stevens, A. J., *J. Catal.* **37**, 179 (1975).
20. Gasser, R. P. H., Jackson, G. V., and Rolling, F. E., *Surface Sci.* **52**, 199 (1975).
21. Hendriksen, B. A., Pearce, D. R., and Rudham, R., *J. Catal.* **24**, 82 (1972).
22. Borello, E., Gatta, G. D., Fubini, B., Morterra, C., and Venturello, G., *J. Catal.* **35**, 1 (1974).
23. Heiba, E. I., and Landis, P. S., *J. Catal.* **3**, 471 (1964).
24. Beynon, J. H., Fontaine, A. E., and Lester, G. R., *Int. J. Mass. Spectrom. Ion Optics.* **1**, 1 (1968).
25. Lifshitz, C., Shapiro, M., and Sternberg, R., *Israel J. Chem.* **7**, 391 (1969).
26. Redhead, P. A., *Vacuum* **12**, 203 (1962).
27. Ehrlich, G., *J. Appl. Phys.* **32**, 4 (1961).
28. Cvetanovic, R. J., and Amenomiya, Y., *Adv. Catal.* **17**, 103 (1967).
29. Peri, J. B., *J. Phys. Chem.* **69**, 211, 220 (1965).